

# Role of Sperm Sulfogalactosylglycerolipid in Mouse Sperm-Zona Pellucida Binding<sup>1</sup>

Dawn White,<sup>3</sup> Wattana Weerachatanukul,<sup>3</sup> Bart Gadella,<sup>4</sup> Nuanthip Kamolvarin,<sup>3</sup> Mayssa Attar,<sup>3</sup> and Nongnuj Tanphaichitr<sup>2,3</sup>

Loeb Health Research Institute,<sup>3</sup> Hormones/Growth/Development Group, Human In Vitro Fertilization Program, Ottawa Hospital at Civic Campus, and Departments of Obstetrics/Gynecology and Biochemistry/Microbiology/Immunology, University of Ottawa, Ottawa, Ontario, Canada K1Y 4E9  
Department of Biochemistry and Cell Biology,<sup>4</sup> Faculty of Veterinary Medicine, Institute of Biomembranes, Utrecht University, Utrecht, The Netherlands

## ABSTRACT

Sulfogalactosylglycerolipid (SGG) is the major sulfoglycolipid of mammalian male germ cells. Like other sulfoglycolipids, SGG is believed to be involved in cell-cell/extracellular matrix adhesion. Specifically, we investigated whether sperm SGG played a role in sperm-egg interaction. Initially, we produced an affinity-purified, rabbit polyclonal immunoglobulin (Ig) G antibody that specifically recognized SGG (anti-SGG). Indirect immunofluorescence using anti-SGG IgG localized SGG to the convex and concave ridges and the postacrosome of the mouse sperm head. Pretreatment of sperm with anti-SGG IgG/Fab inhibited sperm-zona pellucida (ZP) binding *in vitro* in a concentration-dependent manner (to a maximum of 62%). This inhibition was observed at the level of primary binding. Sperm treated with anti-SGG IgG underwent the spontaneous and ZP-induced acrosome reaction at the same rate as control sperm treated with preimmune rabbit serum IgG. Fluorescently labeled SGG liposomes were shown to associate specifically with the egg ZP, whereas fluorescently labeled liposomes of galactosylglycerolipid (SGG's parental lipid) and phosphatidylserine (negatively charged like SGG) did not. Furthermore, coincubation of SGG liposomes with sperm and isolated ZP inhibited sperm-ZP binding in a concentration-dependent manner. These results strongly suggest an involvement of sperm SGG in direct binding to the ZP.

fertilization, ovum, sperm

## INTRODUCTION

Mammalian sperm-egg interaction that leads to fertilization is initiated when sperm bind to the egg extracellular sulfoglycoprotein matrix, the zona pellucida (ZP) [1, 2]. In all mammals studied, the ZP consists of only a few sulfoglycoproteins [2], and in mice, ZP3 (83 kDa) and ZP2 (120 kDa) act as primary and secondary sperm receptors, respectively [2]. The *O*-linked oligosaccharides of mouse ZP3 play a major role in carbohydrate-protein interaction during sperm-ZP binding [2, 3], although the significance of the *N*-linked oligosaccharides of these ZP proteins has

also been addressed recently [4, 5]. The importance of the nonreducing  $\alpha$ -linked galactose residues of mouse ZP3 oligosaccharides in sperm-ZP binding has been described [2, 6], whereas the presence of  $\alpha$ -fucose residues in ZP3 oligosaccharides has been postulated to enhance high-affinity sperm binding [6]. In addition,  $\beta$ -*N*-acetylglucosamine and  $\alpha$ -mannose are two other ZP sugar residues implicated in zona binding through their interaction with sperm surface glycosyltransferases (i.e., sperm  $\beta$ -galactosyltransferase [7]; sperm  $\alpha$ -fucosyltransferase [8]) and glycohydrolases (i.e., sperm  $\alpha$ -mannosidase [9]), respectively. These sperm enzymes act as ligands conjugating sperm to the ZP. In addition to all the sugar residues mentioned, sulfated sugar residues, perhaps on both the ZP and the sperm surface, have been suggested to be involved in sperm-ZP binding [3, 10] based on the finding that polysulfated molecules, such as dextran sulfate, chondroitin sulfate B, fucoidan, and suramin [11–14], inhibit sperm-ZP binding *in vitro*.

Sulfogalactosylglycerolipid (SGG; Fig. 1) is the sulfoglycolipid to which sulfolipid-immobilizing protein-1 (SLIP1), a ZP-binding protein [15], binds specifically *in vitro* [16]. It is the major sulfoglycolipid of mammalian germ cells and sperm (~10 mol% of total lipids) and a minor component in the white matter of the brain (0.2 mol%), but it is absent in other somatic tissues. Structurally, SGG is related to sulfogalactosylceramide (SGC; Fig. 1), a sulfoglycolipid present mainly in the myelin sheath and epithelial cells as well as in the male germ cells of lower vertebrates and certain mammals [17, 18]. Sulfogalactosylglycerolipid is synthesized in zygote spermatocytes [19]. Throughout spermatogenesis, sperm maturation, and the initial stage of *in vitro* sperm capacitation, SGG is not desulfated [16, 20, 21], suggesting that its exposed sulfate moiety may be relevant in sperm-egg interaction.

Like other glycolipids, both SGG and SGC may be involved in cell-cell/extracellular matrix adhesion via the interaction of their galactosyl sulfate moiety with binding ligands [22]. Sulfogalactosylglycerolipid binds several adhesive glycoproteins, including laminin, thrombospondin, and von Willebrand factor [23–25]. Both SGG and SGC bind L/P selectin [26], an adhesive protein involved in the lymphocyte-homing event [27]. Pathogenic micro-organisms (e.g., mycoplasmas [28], malaria sporozoites [29]) or subcellular components of viruses/micro-organisms (e.g., gp120 coat protein of human immunodeficiency virus-1 [30]) also interact with SGG and/or SGC. Considering SGG's ability to interact with various glycoproteins and its localization in both rat and mouse sperm heads to the same region as SLIP1 [15, 31, 32], we postulated that SGG may also be involved in sperm-egg interaction. This report describes three approaches for demonstrating that SGG, especially its sulfate moiety, is significant for sperm-ZP binding. First, a polyclonal anti-SGG IgG antibody was generated and used to mask SGG on the surface of mouse sperm, which were then

<sup>1</sup>Supported by grants from the Medical Research Council Canada (MT-10366) and the Rockefeller Foundation. D.W. is a recipient of the Dimitri N. Chorafas Award (1997) and Norman Barwin Scholarship, Planned Parenthood Federation of Canada (1998–1999). W.W. is an awardee of a graduate study scholarship from the National Science and Technology Development Agency of Thailand. B.G. is supported by the Royal Dutch Academy of Sciences and Arts (KNAW).

<sup>2</sup>Correspondence: Nongnuj Tanphaichitr, Loeb Health Research Institute, 725 Parkdale Ave., Ottawa, ON, Canada K1Y 4E9. FAX: 613 761 5365; e-mail: ntanphaichitr@lri.ca

Received: 29 November 1999.

First decision: 20 December 1999.

Accepted: 17 February 2000.

© 2000 by the Society for the Study of Reproduction, Inc.

ISSN: 0006-3363. <http://www.biolreprod.org>

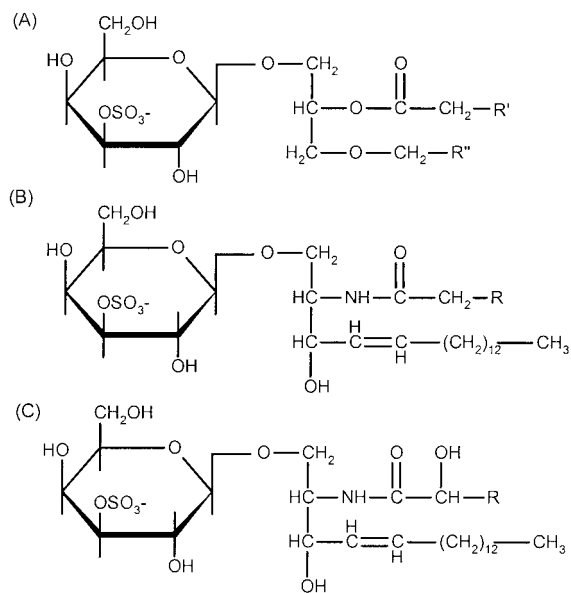


FIG. 1. Chemical structure of SGC (A), nonhydroxylated SGC (B), and  $\alpha$ -hydroxylated SGC (C). In all mammalian species studied, both *sn*-1 alkyl (R'') and *sn*-2 acyl (R') chains of SGC are mainly 16:0 [18]. In contrast, SGC's acyl chain (R) is variable, being mainly 24:1 in bovine brain [34].

tested *in vitro* for their ZP-binding ability. Second, zona-intact mouse eggs and isolated ZP were examined for their ability to bind fluorescently labeled SGC liposomes. Finally, the *in vitro* sperm-ZP binding assay was performed in the presence of SGC liposomes to test the ability of exogenous sulfoglycolipid to compete with endogenous sperm SGC in binding to the ZP.

## MATERIALS AND METHODS

### Gamete Preparation

Both male and female mice were acquired, retained, killed, and used in this study with approval from the local Animal Care Committee. Motile sperm were prepared by two-step Percoll gradient centrifugation of caudal epididymal and vas deferens sperm collected from CD-1 male mice as described elsewhere [15, 21]. Cumulus masses containing mature eggs were retrieved from the oviducts of superovulated CF-1 female mice, and zona-intact eggs were obtained after dissociation of cumulus cells by hyaluronidase [33]. Krebs-Ringer bicarbonate medium buffered with HEPES (119.4 mM NaCl, 4.8 mM KCl, 1.7 mM CaCl<sub>2</sub>, 1.2 mM KH<sub>2</sub>PO<sub>4</sub>, 1.2 mM MgSO<sub>4</sub>, 25 mM sodium lactate, 1 mM sodium pyruvate, 5.6 mM glucose, 28  $\mu$ M phenol red, 4 mM NaHCO<sub>3</sub>, and 21 mM HEPES, pH 7.4) and supplemented with 0.3% BSA (KRB-HEPES-BSA) was used to handle gametes in air, whereas KRB (composed of the same ingredients as KRB-HEPES, except that 25.1 mM NaHCO<sub>3</sub> was used as a buffering component instead of 4 mM NaHCO<sub>3</sub> and 21 mM HEPES) supplemented with 0.3% BSA (KRB-BSA) was used for all gamete functional studies unless stated otherwise.

Fertilized mouse eggs and two-cell mouse embryos were collected from mated female mice following the method described by Hogan et al. [33]. Ovarian ZP were prepared following the method described by Tanphaichitr et al. [15].

### Liposome Preparation

All lipids used in our studies were purchased from Sigma Chemical Co. (St. Louis, MO) unless stated otherwise. Multilamellar liposomes were prepared in PBS or culture medium according to the method described by Attar et al. [34] and were sized using a Submicron Particle Sizer (Model 370; Nicomp Particle Sizing Systems, Santa Barbara, CA) (diameter range, 10–4000 nm with Gaussian distribution; average diameter, 1000 nm). Unilamellar vesicles of 200 nm in diameter were then prepared by extruding these multilamellar vesicles through a polycarbonate filter (pore size, 200 nm) mounted in the LipoFast mini-extruder (Avestin, Inc., Ottawa, ON, Canada) [35].

### Immunization of Rabbits with SGC-Containing Liposomes

To generate an IgG antibody against SGC, we followed the method of Zalc et al. [36], which involved direct, intravenous immunization of sulfoglycolipid-containing liposomes without any adjuvant into the ear vein of New Zealand white female rabbits. Because SGC, a structural analogue of SGG, is commercially available and every anti-SGC antibody generated cross-reacts with SGC and vice versa [30, 37–41], we used SGC-containing liposomes as the immunogen. The SGC-containing multilamellar liposomes (consisting of bovine brain SGC [hydroxy and nonhydroxy]/palmitoylcholine phosphatidylcholine [POPC]/cholesterol, 7:24:64, w/w/w) were prepared in PBS (see above). Control liposomes consisting of POPC/cholesterol (3:8, w/w) were prepared similarly. An aliquot of each liposome preparation (1 ml, consisting of 4.75 mg total lipid) was injected twice weekly over a 6-wk period into the rabbit's ear vein. Two rabbits (R2 and R3) were immunized with the SGC-containing liposomes, and a third rabbit (R1) was injected with the POPC/cholesterol liposomes. Serum was collected before the liposome injection once a week. Preimmune serum was collected before any injections.

Rabbit blood was allowed to clot by incubating at 37°C for 1 h, and then at 4°C overnight. The serum, which was collected from the clotted blood by centrifugation (500  $\times$  g at 4°C for 15 min), was then complement-inactivated (56°C for 1 h) before storage at –70°C. The serum was serially diluted in TBS (154 mM NaCl, 100 mM Tris-HCl, pH 7.4) supplemented with 2% BSA for the ELISA.

The use and maintenance of the three rabbits in this study was approved by the local Animal Care Committee.

### ELISA

The lipid mixture (SGC/POPC/cholesterol, 10:1:1, w/w/w; or POPC/cholesterol [control lipid], 1:1, w/w) was dissolved in chloroform, dried under nitrogen, and then redissolved in ethanol at 10  $\mu$ g/ml. After sonication, 1  $\mu$ g of the lipid solution was dispensed into each well of a 96-well, flat-bottomed Linbro culture plate (ICN Biomedical, Flow Lab, ON, Canada). The plate was air-dried overnight at 22°C and then kept in a desiccator until use.

Each well of the plate was blocked with 200  $\mu$ l of TBS-2% BSA, incubated at 37°C for 1 h under moisture, washed five times with TBS-0.2% BSA, and dried. Diluted serum (100  $\mu$ l) was added into each well, incubated, and washed in the same manner as described for the blocking step. Secondary antibody, horseradish peroxidase (HRP)-conjugated goat antirabbit IgG or IgM (Southern Biotechnology Associates, Inc., Birmingham, AL) was added to each well (100  $\mu$ l, 1:4000 dilution), incubated, and washed likewise.

Bound antibodies were revealed using an *o*-phenylenediamine dihydrochloride (OPD) colorimetric assay according to the manufacturer's protocol (Sigma). Color intensity was measured at  $A_{490}$ .

Three negative control wells were included in the ELISA: 1) blank control (no serum/antiserum), 2) preimmunization control (preimmune rabbit serum [PRS]), and 3) immunization control (serum from rabbit R1 immunized with SGC-depleted liposomes). To obtain the antiserum titer, the ELISA was performed three times on different days. The highest serum dilution that gave an absorbance reading ( $A_{490}$ ) two- to threefold higher than the corresponding diluted preimmune serum was selected. The selected values were averaged from the three days, and the titer was then calculated according to the following equation: End point dilution titer =  $[(A_x - A_{\text{control}}) \times \text{dilution factor}] / A_{\text{control}}$  where  $A_x$  is the average  $A_{490}$  of the test serum and  $A_{\text{control}}$  is the average  $A_{490}$  of the preimmune serum.

#### *Immunodetection of Specific Reactivity of the Antibody Produced Against the SGC-Containing Liposomes on TLC Plates by High-Performance Thin-Layer Chromatography*

Immunological detection of glycolipids was performed following the method described by Kniep and Muhlrath [42], with some modifications [41]. Briefly, 5 nmol of each purified lipid (SGC, hydroxy and nonhydroxy), galactosylceramide (GC; hydroxy and nonhydroxy, prepared according to the method described by Van der Pal et al. [43]), SGG and galactosylglycerolipid (GG; prepared by acidic desulfation of SGG according to the method described by Gadella et al. [44]), monogalactosyldiacylglycerol (MGDG; isolated from spinach chloroplasts according to the method described by Van't Hof et al. [45]), cholesterol sulfate, phosphatidylcholine (PC), phosphatidylserine (PS), phosphatidylethanolamine (PE), phosphatidic acid (PA), and sphingomyelin (SM; isolated according to the method described by Brouwers et al. [46]) was spotted onto two plastic-backed, silica gel, high-performance thin-layer chromatography (HPTLC) plates (Baker Inc., Phillipsburg, NJ), which were then developed with chloroform/methanol/water (65:25:4, v/v/v) and dried. On one plate, all glycolipids and cholesterol sulfate were visualized by orcinol charring [47] and identified based on their known  $R_f$  values. The other plate was processed for immunostaining using our anti-SGC antiserum at a 1:1000 dilution and was detected with HRP-conjugated protein A/G at a 1:1000 dilution.

#### *Preparation of Anti-SGC/SGG IgG Antibody and Affinity-Purified Anti-SGG IgG Antibody*

The IgG fraction of the antiserum from the immunized rabbits R2 and R1 and preimmune serum was precipitated with 50% saturated ammonium sulfate (pH 7.0) [48] and then further purified using the Immuno Pure Immobilized Protein A Affinity Pak Column (Pierce, Rockford, IL). The fractions containing IgG were pooled, lyophilized, and reconstituted in PBS.

The anti-SGG IgG antibody was affinity purified from the antiserum IgG of rabbit R2 using an SGG affinity matrix (kindly provided by Dr. C.A. Lingwood, Hospital for Sick Children, University of Toronto, Toronto, ON, Canada) following the method described by Tanphaichitr et al. [49]. Fab fragments of affinity-purified anti-SGG IgG were then generated using the Immuno Pure Fab Preparation kit (Pierce).

#### *Indirect Immunofluorescence of Sperm with Affinity-Purified Anti-SGG IgG*

Percoll gradient centrifuged (PGC) mouse sperm were capacitated in KRB-0.3% BSA for 30 min (5%  $\text{CO}_2$  at 37°C) and washed twice with PBS. The PGC sperm were used either live or prefixed with 4% paraformaldehyde in PBS containing 320 mM sucrose (room temperature for 30 min) for indirect immunofluorescence (IIF) with anti-SGG IgG. Sperm were incubated with affinity-purified anti-SGG IgG (10  $\mu\text{g}/\text{ml}$  at 37°C for 30 min), which was followed by two washes with PBS. The sperm were then treated (37°C for 30 min) with 100  $\mu\text{g}/\text{ml}$  goat antirabbit IgG conjugated to Cy3, which was prepared using a kit produced by Biological Detection Systems (Pittsburgh, PA), and then washed twice again with PBS. Control sperm samples were incubated with either an equal amount of PRS IgG followed by the same secondary antibody or without the primary antibody.

In addition, IIF of live PGC sperm was performed using rabbit R1 IgG (10  $\mu\text{g}/\text{ml}$ ) and Cy3-conjugated antirabbit IgG. All sperm samples were observed using a Zeiss epifluorescent IM35 inverted microscope.

#### *In Vitro Mouse Sperm-Egg Binding Assay*

Percoll gradient centrifuged sperm were suspended in KRB-BSA to a final concentration of  $10^7/\text{ml}$ , then treated at 37°C (5%  $\text{CO}_2$  for 30 min) with affinity-purified anti-SGG IgG or Fab (0.5–70 or 0.6–6.7  $\mu\text{g}/\text{ml}$ , respectively) or rabbit R1 IgG (70  $\mu\text{g}/\text{ml}$ ). Control samples were treated with 70  $\mu\text{g}/\text{ml}$  PRS IgG or 6.7  $\mu\text{g}/\text{ml}$  PRS Fab. Control, antibody-treated, and untreated sperm samples were then incubated with unfertilized, ovulated, zona-intact mouse eggs. Sperm bound to the egg ZP were counted using the method described by Tanphaichitr et al. [15].

In an alternate set of experiments, isolated ovarian ZP were incubated with PGC sperm, precapacitated in KRB-BSA, in 60- $\mu\text{l}$  droplets of KRB supplemented with 0.1% polyvinylpyrrolidone (KRB-PVP) at 37°C (5%  $\text{CO}_2$  for 10 min) following the method described by Tanphaichitr et al. [15] in the presence or absence of unilamellar SGG liposomes (diameter, 200 nm) or unilamellar PS liposomes of the same size. Sperm-ZP complexes were then washed in KRB-PVP droplets four times before ZP-bound sperm were counted.

Differences in the number of sperm bound per egg in the control and experimental samples were analyzed using ANOVA.

#### *Binding of Fluorescently Labeled SGG/PS/GG-Containing Liposomes to Egg ZP*

Liposomes of experimental lipids (SGG, PS, and GG) were fluorescently labeled by including a small amount of lissamine rhodamine B 1,2-dihexadecanoyl-*sn*-glycero-3-phosphoethanolamine (*N*-Rh-PE; Molecular Probes Inc., Eugene, OR) during multilamellar liposome preparation [34] in PBS (experimental lipid/*N*-Rh-PE, 70:1 molar ratio) (described earlier). The liposomes (SGG, PS, or GG) were resuspended at a concentration of 1 mg/ml of total lipid, and 0.5  $\mu\text{g}$  was used for incubation at 37°C (5%  $\text{CO}_2$  for 15 min) with 20 unfertilized or fertilized zona-intact eggs, isolated ovarian ZP, or two-cell embryos in a 60- $\mu\text{l}$  drop of PBS with 0.1% PVP (PBS-PVP), with or without 10 mM  $\text{Ca}^{2+}$ . Alternatively, ZP were prewashed overnight at 37°C in PBS-PVP containing 10 mM EDTA before coincubating

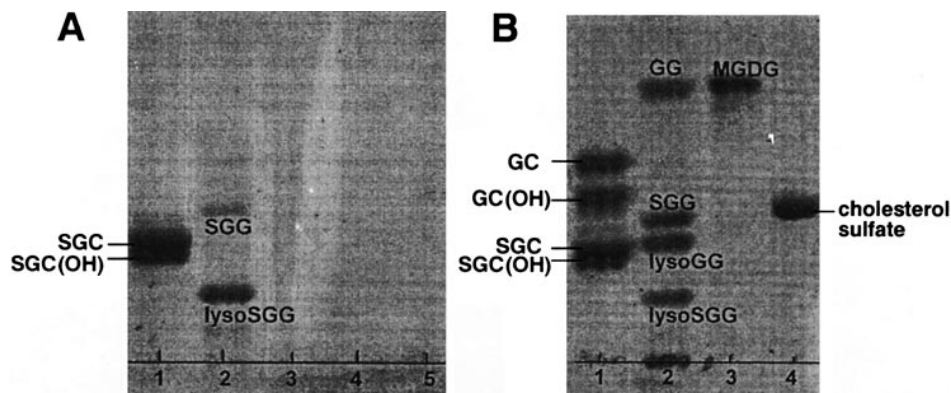


FIG. 2. Specificity of antiserum from rabbit R2, immunized with SGC-containing liposomes. **A**) Immunostained plate showing cross-reactivity of antiserum from rabbit R2 with SGG, lyso-SGG, and SGC (hydroxy and nonhydroxy). **B**, Orcinol charred plate showing the positions of developed lipids, except for phospholipids (lane 5), which cannot be detected by this method.

with the fluorescent SGG liposomes. In addition, unilamellar 200-nm liposomes, generated from the multilamellar fluorescent liposomes (described earlier), were used for egg, ZP, or embryo binding. A liposome competition assay was also performed with both multilamellar and 200-nm liposomes by incubating zona-intact eggs with 0.5  $\mu\text{g}$  of fluorescent SGG liposomes with 100  $\mu\text{g}$  of nonfluorescent SGG/PE (70:1 molar ratio) liposomes under the same conditions. Eggs, ZP, or embryos were subsequently washed in PBS-PVP, mounted in small volume on a slide, and topped with a coverslip cushioned with Nivea cream. Fluorescence was observed using a Zeiss IM35 inverted epifluorescent microscope.

Binding of pure SGG liposomes (multilamellar and unilamellar) to zona-intact eggs and isolated ZP was also investigated following the same conditions as described earlier for fluorescent SGG liposomes. Detection of SGG bound to the egg ZP was performed using affinity-purified anti-SGG IgG (50  $\mu\text{g}/\text{ml}$ ) followed by Cy3-goat antirabbit IgG (100  $\mu\text{g}/\text{ml}$ ).

#### Assessment of Acrosome Integrity

Ovarian mouse ZP were solubilized following a modification of the method described by Ward et al. [50]. Briefly, ZP were heat solubilized at 20 ZP/ $\mu\text{l}$  at 60°C for 60 min and then concentrated to 100 ZP/ $\mu\text{l}$  using a Microcon 30 (Amicon Inc., Beverly, MA). Percoll gradient centrifuged sperm (5–10  $\times 10^6/\text{ml}$ ) treated with 50  $\mu\text{g}/\text{ml}$  of affinity-purified anti-SGG IgG or PRS IgG (control) were divided into two samples. One sample was evaluated for spontaneous acrosome reaction, and the other was treated with solubilized ZP at a final concentration of 10 ZP/ $\mu\text{l}$  at 37°C (5%  $\text{CO}_2$  for 30 min) to assess ZP-induced acrosomal exocytosis. Sperm samples were fixed and stained with Co-

massie Blue following the method described by Bleil and Wassarman [51] to assess the acrosomal status. Two-hundred sperm from each sample were evaluated using a Zeiss Axioskop light microscope at  $\times 400$  magnification.

## RESULTS

### Properties of the Polyclonal Rabbit Antibody Generated Against SGC-Containing Liposomes

Production of a polyclonal antibody reacting with SGG that was IgG was essential for functional studies of sperm SGG. The ELISA revealed that antisera from both rabbits (R2 and R3) immunized with these SGC-containing liposomes showed a maximum titer of 90 000 or greater between Days 35 and 42. When secondary antibody specific to rabbit IgM was used in place of IgG, no titer was observed with these antisera, indicating that the antibody produced was enriched in IgG. The ELISA also showed that serum from the control rabbit (R1) injected with POPC/cholesterol did not cross-react with SGC/POPC/cholesterol liposomes.

Using an HPTLC overlay technique [41, 42], the antiserum from rabbit R2 showed specific cross-reactivity with SGG, lyso-SGG, and SGC (both hydroxy and nonhydroxy subclasses), but not with the parental molecules GG and GC (both hydroxy and nonhydroxy subclasses), as well as the other lipids tested, including cholesterol sulfate, MGDG, PC, PS, PE, PA and SM (Fig. 2A). Lipids on the duplicate thin-layer chromatogram were visualized by orcinol charring, except for phospholipids (PC, PS, PE, PA, and SM; Fig. 2B). The cross-reactivity of our antibody with SGG was expected, because all previous antibodies produced against SGC also cross-react with SGG [30, 37–41]. Therefore, we named the antibody anti-SGC/SGG. Anti-SGC/SGG did not cross-react with mouse sperm proteins as assessed by immunoblotting (data not shown). The yield of affinity-purified anti-SGG IgG prepared by subjecting the polyclonal anti-SGC/SGG IgG (from rabbit R2) to SGG affinity column chromatography was approximately 1%.

### Immunolocalization of SGG in Mouse Sperm

Indirect immunofluorescence of aldehyde fixed PGC mouse sperm (Fig. 3A) using our affinity-purified anti-SGG IgG revealed fluorescent staining mainly at the convex ridge of the sperm head. In approximately 30% of sperm, additional staining was observed in the postacrosomal region (Fig. 3A). In contrast, IIF of live PGC sperm using

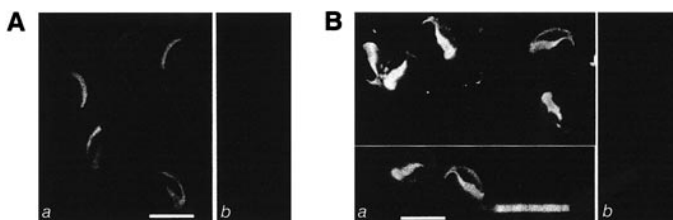


FIG. 3. Indirect immunofluorescence of mouse PGC sperm with affinity-purified anti-SGG IgG. **A**) Aldehyde-fixed sperm exposed to affinity-purified anti-SGG IgG (panel a) or PRS IgG (panel b). **B**) Live sperm exposed to affinity-purified anti-SGG IgG (panel a) or PRS IgG (panel b). Bar = 10  $\mu\text{m}$ .

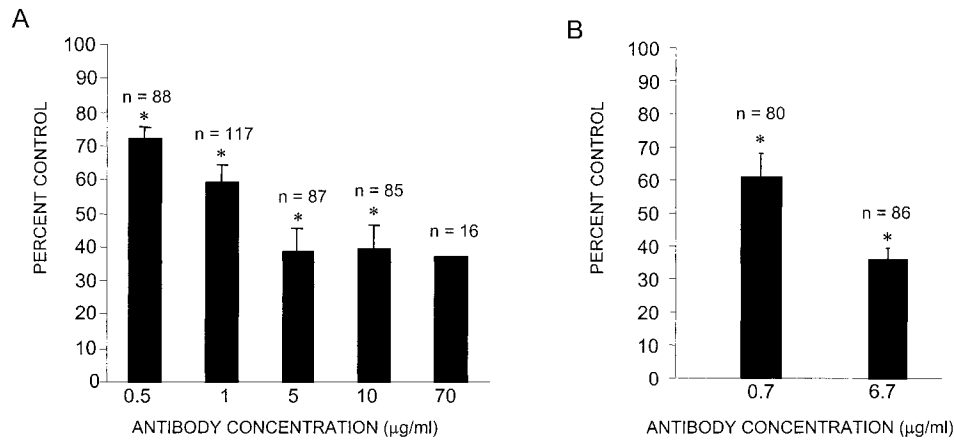


FIG. 4. Inhibition of mouse sperm-ZP binding by pretreatment of sperm with affinity-purified anti-SGG IgG (A) or Fab (B). Except for data regarding the 70  $\mu\text{g/ml}$  anti-SGG IgG sample, all data are expressed as mean  $\pm$  SD of percentage control of averages from three or more experiments. n = Total number of eggs analyzed for each sample; \*significant difference compared with controls.

the same affinity-purified anti-SGG IgG showed fluorescent staining in all sperm at the postacrosome and at the concave and convex ridges of the sperm head. Approximately 15% of live sperm showed additional staining in the midpiece (Fig. 3B). The IIF of live PGC sperm using IgG (100  $\mu\text{g/ml}$ ) from rabbit R1 revealed two punctate fluorescent staining patterns that were dissimilar to those using affinity-purified anti-SGG. The first pattern appeared as a thick band in the sperm head convex ridge in 70% of the PGC sperm population. The remainder of the PGC sperm population showed a fluorescent staining in the postacrosomal region (as a thick band) as well as in the midpiece (data not shown).

#### *Anti-SGG-Pretreated Sperm Had Decreased ZP-Binding Ability*

Because we localized SGG to areas of the mouse sperm head involved in ZP binding (i.e., the sperm head convex ridge and the postacrosome [1, 52]), we further evaluated whether sperm SGG played a role in this gamete interaction. The SGG on capacitated PGC mouse sperm was masked with affinity-purified anti-SGG IgG before coin-cubation with zona-intact eggs. Because SGG is present at a substantial level in mouse sperm (i.e., 10% of total lipids or 0.6 nmole/ $10^6$  sperm) and  $10^6$  PGC sperm/ml was required for the in vitro gamete-binding assay, approximately 0.3 nmol in a 60- $\mu\text{l}$  gamete droplet (or  $\sim 50$   $\mu\text{g/ml}$ ) of bivalent anti-SGG IgG would be needed to bind most SGG on the PGC sperm. Therefore, affinity-purified anti-SGG IgG was used at microgram-per-milliliter concentrations for sperm treatment. Results shown in Figure 4A, indicate that pretreatment of sperm with affinity-purified anti-SGG IgG reduced sperm-ZP binding ( $P < 0.005$  vs. control) in a concentration-dependent manner, and that inhibition reached 62% of the control at 5  $\mu\text{g/ml}$  of affinity-purified anti-SGG IgG. Higher concentrations of antibody had no greater inhibitory effect (e.g., 10 and 70  $\mu\text{g/ml}$ ). The control, in which sperm were pretreated with PRS IgG at 70  $\mu\text{g/ml}$ , had an average of  $26.4 \pm 5.5$  sperm bound/egg. These values were similar to that obtained when untreated sperm were used for gamete coin-cubation. In addition, sperm pretreated with 70  $\mu\text{g/ml}$  of rabbit R1 IgG, which interacted with a surface antigen localized to the sperm head convex ridge region in 70% of PGC sperm, could bind to the ZP to the same extent as untreated sperm. To further

ensure these results were, indeed, not caused by IgG-antibody-induced steric hindrance of gamete interaction, affinity-purified monovalent anti-SGG Fab at concentrations of 0.7 and 6.7  $\mu\text{g/ml}$  (equivalent to 1 and 10  $\mu\text{g/ml}$  of affinity-purified anti-SGG IgG) were used for sperm treatment. Sperm pretreated with 6.7  $\mu\text{g/ml}$  PRS Fab, serving as a control, bound to the egg at the level of  $29.1 \pm 8.5$  sperm/egg. Results, shown in Figure 4B, revealed that affinity-purified anti-SGG Fab inhibited sperm-ZP binding at the same level (61% and 36% of control at 0.7 and 6.7  $\mu\text{g/ml}$ , respectively) as that observed with equivalent concentrations of affinity-purified anti-SGG IgG (58% and 38% of control at 1 and 10  $\mu\text{g/ml}$ , respectively).

Inhibition of sperm-ZP binding to approximately 56% of the control value was also observed when affinity-purified anti-SGG IgG-treated sperm (50  $\mu\text{g/ml}$ ) were incubated with eggs (n = 92) for only 10 min (vs. the conventional 30 min). Control sperm treated with an equivalent concentration of PRS IgG bound  $15.1 \pm 2.1$  sperm/egg (n = 70). At this 10-min time-point, sperm-ZP binding is at the primary stage [53]. It is possible that sperm SGG might be involved in the primary sperm-ZP binding, although direct binding of SGG to ZP3 needs to be shown for definitive inference [2]. Furthermore, our results did not exclude the possibility that sperm SGG may also participate in secondary sperm-ZP binding.

#### *SGG Liposomes Bound to the ZP of Unfertilized Eggs*

To further validate that sperm SGG was involved in sperm-ZP interaction, direct binding of SGG to the ZP was demonstrated. Figure 5A (panels a–d) clearly demonstrates that fluorescently labeled SGG liposomes (SGG/N-Rh-PE) (diameter, 200 nm) bound to isolated ovarian ZP and unfertilized ovulated egg ZP. In contrast, fluorescently labeled PS liposomes, which were negatively charged like SGG/N-Rh-PE liposomes, did not bind to the unfertilized egg ZP (Fig. 5A, panel e), nor did fluorescently labeled liposomes of GG, the parental lipid of SGG (Fig. 5A, panel f). Furthermore, an excess of nonfluorescent SGG/PE liposomes could block binding of SGG/N-Rh-PE liposomes to the unfertilized egg ZP (Fig. 5A, panel g). Liposomes constructed with N-Rh-PE alone did not stain the egg ZP. The same results as shown in Figure 5 were also obtained when multilamellar vesicles of fluorescent liposomes (SGG, GG, or PS) were used in place of the corresponding 200-nm uni-

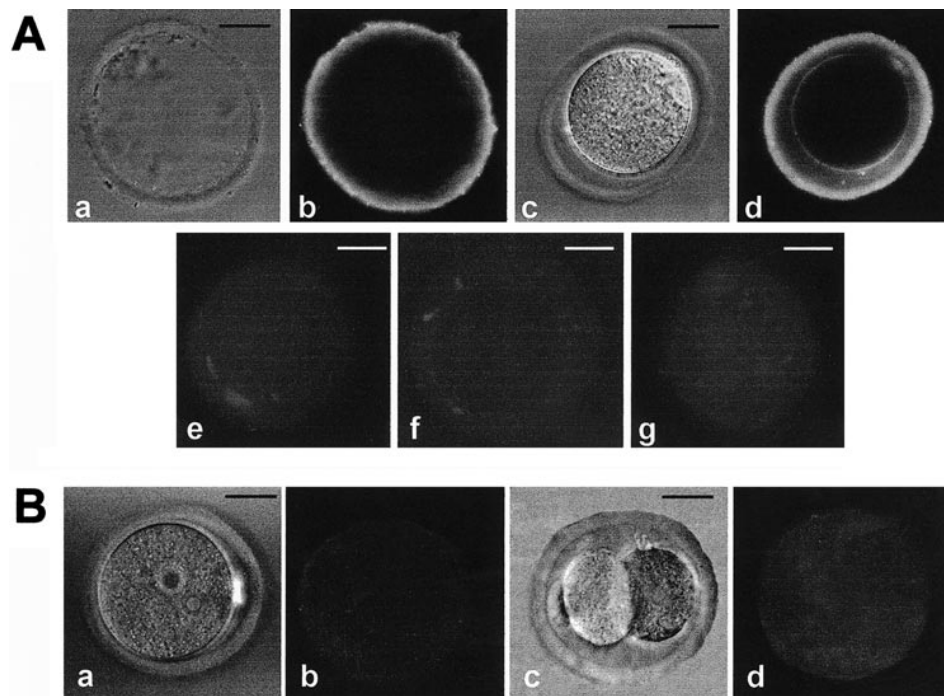


FIG. 5. Fluorescent staining of isolated ovarian ZP, unfertilized zona-intact eggs, and zygotes and two-cell embryos by fluorescently labeled SGG liposomes. **A**) The ZP (panels a and b) and unfertilized zona-intact eggs (panels c and d) were incubated with SGG/*N*-Rh-PE liposomes; unfertilized zona-intact eggs were incubated with PS/*N*-Rh-PE (panel e) liposomes, GG/*N*-Rh-PE (panel f), or SGG/*N*-Rh-PE with SGG/PE (200× of SGG/*N*-Rh-PE) (panel g). All panels are fluorescent micrographs, except for panels a and c, which are corresponding phase-contrast micrographs of panels b and d, respectively. Note fluorescent staining of the isolated ZP and the ZP and plasma membrane of unfertilized eggs exposed to SGG/*N*-Rh-PE (panels b and d), whereas eggs incubated with other liposomes did not show fluorescent staining. **B**) Zygotes (panels a and b) and two-cell embryos (panels c and d) were incubated with SGG/*N*-Rh-PE liposomes. Panels a and c are phase-contrast images of panels b and d, respectively. Note the minimal fluorescent staining for SGG/*N*-Rh-PE on the embryo ZP (panels b and d). Bar = 20 μm.

lamellar vesicles (data not shown), suggesting that SGG binding to the ZP was not dependent on liposome size. In addition, fluorescent SGG liposomes bound to the ZP to the same extent, regardless of whether  $\text{Ca}^{2+}$  (10 mM) was present or absent in the ZP droplet. Furthermore, prewashing of the ZP with EDTA-containing PBS did not diminish their affinity to the fluorescent SGG liposomes (data not

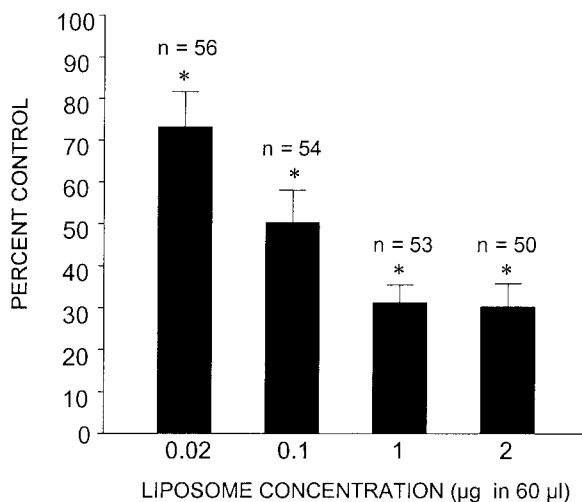


FIG. 6. Inhibition of sperm-ZP binding by exogenous SGG liposomes. All data were expressed as number of sperm bound/ZP  $\pm$  SD. Sperm-ZP coincubates treated with PS liposomes (2 μg in the 60-μl gamete droplet) served as a control. All liposomes used were unilamellar (diameter, 200 nm). n = Total number of eggs analyzed for each sample; \*significant difference compared with control.

shown). These data, considered together, suggest that external  $\text{Ca}^{2+}$  is not essential for SGG-ZP interaction. In addition, to exclude any possibility that *N*-Rh-PE, although present in a very small amount in the fluorescently labeled liposomes, may influence the ability of SGG to bind to the ZP, pure SGG liposomes were used for incubation with zona-intact eggs or isolated ovarian ZP, and the detection of their ZP binding was performed using affinity-purified anti-SGG IgG antibody and fluorescently labeled secondary antibody. Positive SGG binding to the ZP was observed in the same manner as when SGG/*N*-Rh-PE was used, whereas zona-intact eggs exposed to only the secondary antibody showed no fluorescent staining (data not shown). Collectively, these results indicate the specificity of SGG binding to the ZP and the importance of the sulfate moiety of this sperm-specific sulfoglycolipid in sperm-ZP binding.

Binding of SGG/*N*-Rh-PE liposomes to the plasma membrane of unfertilized eggs was also observed (Fig. 5A, panel d). Presumably, liposomes having a deformable structure can pass through ZP having a high porosity [54, 55]. Since SLIP1 is present on the egg plasma membrane without its counterpart SGG [56], this would allow its interaction with the permeated SGG/*N*-Rh-PE liposomes.

Unlike the unfertilized egg ZP, the ZP of zygotes or two-cell embryos showed minimal fluorescent staining when the embryos were exposed to SGG/*N*-Rh-PE liposomes. This suggested that the number of SGG-binding ligands on the ZP was reduced as a result of fertilization.

#### Exogenous SGG Liposomes Inhibited Sperm-ZP Binding In Vitro

When 200-nm SGG liposomes (0.01–2 μg) were added to the 60-μl droplets of sperm and ZP coincubates, the num-

ber of sperm bound per egg decreased significantly ( $P < 0.005$  vs. control) in a concentration-dependent manner and reached the plateau of 30% of the control value at 1  $\mu\text{g}$  of SGG (Fig. 6). In contrast, 200-nm PS liposomes (negatively charged like SGG liposomes) when added exogenously (2  $\mu\text{g}$  in the 60- $\mu\text{l}$  droplet) to the sperm-ZP coincubates did not inhibit sperm binding to the ZP compared with the untreated sperm-ZP coincubates (data not shown). Therefore, the sperm-ZP coincubates containing PS liposomes, exhibiting  $24.8 \pm 8.5$  sperm bound per ZP, were used as controls. The inhibition of sperm-ZP binding observed in the sperm-ZP coincubates treated with SGG liposomes presumably resulted from the competition of exogenously added SGG liposomes with sperm SGG in ZP binding.

#### *Lack of Effect of Sperm Treatment with Anti-SGG IgG on the Spontaneous and ZP-Induced Acrosome Reaction and Motility*

Treatment of sperm with affinity-purified anti-SGG IgG (50  $\mu\text{g}/\text{ml}$ ) did not induce the spontaneous acrosome reaction or inhibit the ZP-induced acrosome reaction. The anti-SGG-IgG-treated sperm showed  $6.0\% \pm 4.0\%$  of the total population undergoing a spontaneous acrosome reaction, which was similar to the results observed with 50  $\mu\text{g}/\text{ml}$  PRS-IgG-treated ( $8.37\% \pm 2.1\%$ ) and control untreated ( $8.9\% \pm 4.3\%$ ) sperm samples. Most anti-SGG-treated sperm ( $97.7\% \pm 3.2\%$ ) underwent the acrosome reaction when exposed to heat-solubilized ZP in a similar manner to untreated ( $94.6\% \pm 6.0\%$ ) and PRS-IgG-treated sperm ( $99.3\% \pm 1.2\%$ ). The results suggested that anti-SGG IgG did not interfere with the spontaneous or ZP-induced acrosome reaction.

Sperm treated with affinity-purified anti-SGG IgG/Fab, PRS IgG (70  $\mu\text{g}/\text{ml}$ ), or PRS Fab (6.7  $\mu\text{g}/\text{ml}$ ) had the same motility as untreated sperm ( $\sim 60$ – $80\%$ ).

## DISCUSSION

To our knowledge, this report described for the first time combined results of the localization and physiological functions of sperm SGG, which is the major sulfoglycolipid expressed selectively in mammalian male germ cells [18]. Specifically, SGG was localized mainly to the mouse sperm head. Using anti-SGG IgG/Fab produced in our laboratory to mask sperm SGG, we demonstrated that this sulfoglycolipid was involved in primary sperm-ZP binding. This interpretation was further supported by the results showing direct binding of fluorescently labeled SGG liposomes to the ZP and by inhibition of sperm-ZP binding *in vitro* by excess SGG added exogenously to the sperm-ZP coincubates.

Indirect immunofluorescent studies using affinity-purified anti-SGG IgG revealed the presence of SGG in the mouse sperm head, although the fluorescent staining patterns were different in aldehyde-fixed and live sperm. The staining was mainly at the convex ridge in aldehyde-fixed sperm but at both the convex and concave ridges and the postacrosome in live sperm. In contrast, our previous IIF results (also performed in aldehyde-fixed mouse sperm but using monoclonal anti-SGG IgM) showed SGG fluorescent staining over the entire sperm head anterior [15]. Although aldehyde does not fix most lipids, it cross-links proteins and PE on the sperm surface, and this may retard lipid movement, possibly induced by binding of the lipids' multivalent antibodies. Because IgG is bivalent and IgM is multivalent, the SGG staining pattern of fixed sperm by anti-SGG IgG at the sperm head convex ridge (Fig. 3A) is probably closer

to its original site *in situ* than that of anti-SGG IgM, which may relocalize SGG to the entire sperm head [15]. In live sperm with a fluid membrane, anti-SGG IgG may partially relocalize SGG to the concave ridge and postacrosome (Fig. 3B). Our results and interpretation on SGG relocalization on the mouse sperm head corroborate the previous observation, describing the movement of SGG from the sperm head anterior to the postacrosome, as a result of capacitation in pig sperm [57]. SGG fluorescent staining was also observed in the midpiece of 15% of live sperm but was consistently absent in aldehyde-fixed sperm. The SGG may be localized to the membrane of mitochondria present in the midpiece. Because repeated centrifugation was employed during IIF, 15% of the sperm may have had a damaged plasma membrane, thus allowing antibodies to enter the sperm cell and to react with SGG on the mitochondria. This postulation is supported by our own, unpublished results showing that live PGC sperm, pretreated with 0.05% Triton X-100 to remove plasma membrane before IIF, show SGG fluorescent staining only at the sperm midpiece.

The postacrosome and convex ridge of the mouse sperm head are the two sites documented to interact with the ZP [1, 52]. Our immunofluorescent results, indicating that SGG was localized to these two sites (Fig. 3), prompted us to investigate SGG's role in sperm-ZP binding. Because the anti-SGG antibody we produced was IgG, we expected that pretreatment of sperm with anti-SGG IgG or Fab before coincubation with eggs would specifically mask SGG without confounding steric hindrance. The results shown in Figure 4 demonstrate that sperm SGG directly participated in this gamete interaction, because a decrease in sperm-ZP binding was observed in a concentration-dependent manner after sperm pretreatment with anti-SGG IgG. The decrease did not result from a premature acrosome reaction or impaired sperm motility because of antibody treatment, suggesting that sperm SGG was directly involved in ZP binding. This postulation is further supported by results of the liposome-binding experiments, demonstrating direct interaction of fluorescently labeled SGG with the ZP of unfertilized eggs (Fig. 5A, panels a–d). The absence of ZP fluorescent staining when excess nonfluorescent SGG/PE liposomes were included with SGG/N-Rh-PE liposomes during ZP incubation further indicated specificity of the SGG-ZP binding (Fig. 5A, panel g). In addition, SGG/N-Rh-PE liposomes showed much reduced binding to the ZP of zygotes and two-cell embryos (Fig. 5B), which had lost their ability to bind sperm [1], suggesting that SGG interaction with the ZP was specific to the fertilization process. That sperm-ZP binding was significantly decreased in a concentration-dependent manner when excess SGG liposomes were included in the sperm-ZP coincubates to compete with endogenous sperm SGG in ZP binding (Fig. 6) supports this finding. Collectively, our results strongly suggest the significance of sperm SGG in ZP binding at the fertilization onset, and they corroborate other observations regarding the role of SGG/SGC in cell-cell/extracellular matrix adhesion [22–26, 28–30]. However, maximal inhibition of sperm-ZP binding caused by sperm pretreatment with anti-SGG IgG/Fab or gamete coincubation with SGG liposomes did not reach the background, nonspecific sperm-binding level as observed on the ZP of two-cell embryos (i.e., 5%–20% of control unfertilized eggs [15]). This may be due to the possibility that SGG functions in ZP binding with another molecule(s), which was not perturbed in our experiments.

The lack of binding of GG/N-Rh-PE liposomes to the

egg ZP (Fig. 5A, panel f) suggested the importance of the SGG sulfate moiety in ZP interaction. Our results are consistent with previous findings describing inhibitory effects on sperm-ZP binding by various sulfated glycoconjugates when included in gamete coinocultures [11–13]. Those results could be interpreted to implicate the significance of sulfated sugar residues on ZP oligosaccharides in sperm-ZP interaction [58–60], or they could be construed as resulting from disruption of the interaction between the sulfated sugar residue on sperm (e.g., that of SGG) and a ligand on the ZP. Our results support the latter postulation, although they do not discount the importance of the ZP sulfated sugar residues in this gamete interaction. Our results also support other findings that sulfated sugar residues are important in cell-cell/extracellular interactions. Examples of these sulfated sugar residues include Gal-6-sulfate and GlcNAc-6-sulfate of the *O*-glycan of GlyCam-1 (i.e., a receptor of LL selectin), which participate in the interaction between lymphocytes and endothelial cells during the lymphocyte homing event [61].

Like sperm SLIP1 [62] and  $\beta$ -galactosyltransferase [63], sperm SGG is present in several mammalian species [18]. This argues that SGG's role in ZP binding is common among various sperm species. In fact, our own, unpublished results reveal the importance of human sperm SGG in human ZP binding. Therefore, at least another ZP-binding sperm surface molecule is responsible for the species-specific interaction with the ZP. The molecular mechanism of interaction between sperm SGG and the ZP glycoproteins is still unknown. The sulfate moiety of SGG may interact electrostatically with positively charged amino acids, such as arginine [64], of ZP glycoproteins in a fashion similar to that postulated for the interaction between SGG/SGC and L-selectin [61]. However, because PS/N-Rh-PE liposomes, carrying one negative charge like SGG/N-Rh-PE liposomes, did not bind to the ZP (Fig. 5A, panel e), the postulated mechanism of SGG-ZP electrostatic interaction likely also depends on the conformation of the sulfate and other structural groups of SGG. Alternatively, the galactosyl group of SGG may interact with sugar residues of ZP glycoproteins. This type of carbohydrate-carbohydrate interaction has been documented for other glycolipids, such as that observed in a model system (between SGC and GC) [65] and in a ganglioside-mediated cell-substratum interaction [66]. It should also be noted that SLIP1, like SGG (Fig. 3), is localized to the postacrosome [32] and the convex ridge of the mouse sperm head [15, 32]. Based on the *in vitro* affinity of SGG and SLIP1 [16, 49] and the documented role of sperm SLIP1 in sperm-ZP binding [15, 49], SGG and SLIP1 may act as a complex during this gamete interaction. Similarly, SGG may interact with zonadhesin, another sperm surface protein with ZP affinity, via its von Willebrand factor domain [25, 67], and the complex may work together to bind to the ZP. Because the highest inhibition of sperm-ZP binding was observed in sperm pretreated with 5  $\mu$ g/ml affinity-purified anti-SGG, which is a concentration expected to mask only 10% of total sperm SGG, it is unlikely that all sperm SGG ( $\sim 10^8$  molecules/sperm) would participate in ZP binding. Some SGG may be on the mitochondria, as suggested earlier, although the exact distribution of SGG in sperm subcellular components is not known. A portion of SGG on the sperm surface may also be involved in regulating sperm membrane fluidity, perhaps by interacting with phospholipids or by complexing with  $\text{Ca}^{2+}$ , as suggested from our own thermotropic and pressure-tuning infrared spectroscopy studies using SGG model

membranes [34, 68]. Current work in our laboratory is geared toward understanding potential direct interaction among SLIP1, SGG, and ZP sulfoglycoproteins.

## ACKNOWLEDGMENTS

The authors thank Drs. Euridice Carmona and Morris Kates for their valuable comments and Ms. Terri van Gulik, Ms. Beth Paul, and Mr. Maroun Bou Khalil for help in manuscript preparation.

## REFERENCES

1. Yanagimachi R. Mammalian fertilization. In: Knobil E, Neill JE (eds.), *The Physiology of Reproduction*. New York: Raven Press; 1994: 189–317.
2. Wassarman PM. Mammalian fertilization: molecular aspects of gamete adhesion, exocytosis, and fusion. *Cell* 1999; 96:175–183.
3. Chapman NR, Barratt CLR. The role of carbohydrate in sperm-ZP3 adhesion. *Mol Hum Reprod* 1996; 2:767–774.
4. Yonezawa N, Aoki H, Hatanaka Y, Nakano M. Involvement of *N*-linked carbohydrate chains of pig zona pellucida in sperm-egg binding. *Eur J Biochem* 1995; 233:35–41.
5. Yonezawa N, Mitsui S, Kudo K, Nakano M. Identification of an *N*-glycosylated region of pig zona pellucida glycoprotein ZPB that is involved in sperm binding. *Eur J Biochem* 1997; 248:86–92.
6. Johnston DS, Wright WW, Shaper JH, Hokke CH, Van den Eijnden DH, Joziassse DH. Murine sperm-zona binding, a fucosyl residue is required for a high affinity sperm-binding ligand. *J Biol Chem* 1998; 273:1888–1895.
7. Miller DJ, Macek MB, Shur BD. Complementarity between sperm surface  $\beta$ -1,4-galactosyltransferase and egg-coat ZP3 mediates sperm-egg binding. *Nature* 1992; 357:589–593.
8. Apter FM, Baltz JM, Millette CF. A possible role for cell surface fucosyl transferase (FT) activity during sperm zona-pellucida binding in the mouse. *J Cell Biol* 1988; 107:175a.
9. Cornwall GA, Tulsiani DRP, Orgebin-Crist MC. Inhibition of the mouse sperm surface  $\alpha$ -D-mannosidase inhibits sperm-egg binding *in vitro*. *Biol Reprod* 1991; 44:913–921.
10. Jones R. Interaction of zona pellucida glycoproteins, sulphated carbohydrates and synthetic polymers with proacrosin, the putative egg-binding protein from mammalian spermatozoa. *Development* 1991; 111:1155–1163.
11. Huang TTF, Kosower NS, Yanagimachi R. Localization of thiol and disulfide groups in guinea pig spermatozoa during maturation and capacitation using bimane fluorescent labels. *Biol Reprod* 1984; 31:797–809.
12. O'Rand MG, Widgren EE, Fisher SJ. Characterization of the rabbit sperm membrane autoantigen RSA, as a lectin-like zona binding protein. *Dev Biol* 1988; 129:231–240.
13. Jones R, Williams RM. Identification of zona- and fucoidan-binding proteins in guinea-pig spermatozoa and mechanism of recognition. *Development* 1990; 109:41–50.
14. Jones R, Parry R, Leggio LL, Nickel P. Inhibition of sperm-zona binding by suramin, a potential 'lead' compound for design of new anti-fertility agents. *Mol Hum Reprod* 1996; 2:597–605.
15. Tanphaichitr N, Smith J, Mongkolsirikieart S, Gradil C, Lingwood C. Role of a gamete specific sulfoglycolipid-immobilizing protein on mouse sperm-egg binding. *Dev Biol* 1993; 156:165–175.
16. Lingwood CA. Protein-glycolipid interactions during spermatogenesis. Binding of specific germ cell proteins to sulfatoxygalactosylalkylglycerol, the major glycolipid of mammalian male germ cells. *Can J Biochem Cell Biol* 1985; 63:1077–1085.
17. Hakomori SI. Glycosphingolipids in cellular interaction, differentiation, and oncogenesis. *Annu Rev Biochem* 1981; 50:733–764.
18. Murray RK, Narasimhan R. Glycoglycerolipids of animal tissues. In: Kates M (ed.), *Glycolipids, Phosphoglycerolipids, and Sulfoglycerolipids*. New York: Plenum Press; 1990: 321–361.
19. Lingwood CA. Timing of sulphogalactolipid biosynthesis in the rat testis studied by tissue autoradiography. *J Cell Sci* 1985; 75:329–338.
20. Kornblatt MJ. Synthesis and turnover of sulfogalactoglycerolipid, a membrane lipid, during spermatogenesis. *Can J Biochem* 1979; 57: 255–258.
21. Tanphaichitr N, Smith J, Kates M. Levels of sulfogalactosylglycerolipid in capacitated motile and immotile mouse sperm. *Biochem Cell Biol* 1990; 68:528–535.
22. Roberts DD, Ginsburg V. Sulfated glycolipid and cell adhesion. *Arch Biochem Biophys* 1988; 267:405–415.
23. Roberts DD, Roa CN, Mangani JL, Spitalnik SL, Liotta LA, Ginsberg



- V. Laminin binds specifically to sulfated glycolipids. *Proc Natl Acad Sci U S A* 1985; 82:1306–1310.
24. Roberts DD, Haverstick DM, Dixit VM, Frazier WA, Santoro SA, Ginsburg V. The platelet glycoprotein thrombospondin binds specifically to sulfated glycolipids. *J Biol Chem* 1985; 260:9405–9411.
  25. Roberts DD, Williams SB, Gralnick HR, Ginsburg V. Von Willebrand factor binds specifically to sulfated glycolipids. *J Biol Chem* 1986; 261:3306–3309.
  26. Suzuki Y, Toda Y, Tamatani T, Watanabe T, Suzuki T, Nakao T, Murase K, Kiso M, Hasegawa A, Tadano-Aritomi K, Ishizuka I, Miyasaka M. Sulfated glycolipids are ligands for a lymphocyte homing receptor, L-selectin (LECAM-1), binding epitope in sulfated sugar chain. *Biochem Biophys Res Commun* 1993; 190:426–434.
  27. Laskey LA. The homing receptor (LECAM 1/L selectin): a carbohydrate-binding mediator of adhesion in the immune system. In: Harlan JM, Liu DY (eds.), *Adhesion: Its Role in Inflammatory Disease*. New York: W.H. Freeman and Company; 1992: 43–63.
  28. Lingwood C, Schramayr S, Quinn P. Male germ cell specific sulfogalactosylglycerolipid is recognized and degraded by mycoplasmas associated with male infertility. *J Cell Physiol* 1990; 142:170–176.
  29. Pancake S, Holt G, Mellouk S, Hoffman S. Malaria sporozoites and circumsporozoite proteins bind specifically to sulfated glycoconjugates. *J Cell Biol* 1992; 117:1351–1357.
  30. Harouse JM, Bhat S, Spitalnik SL, Laughlin M, Stefano K, Silberberg DH, Gonzalez-Scarano F. Inhibition of entry of HIV-1 in neural cell lines by antibodies against galactosyl ceramide. *Science* 1991; 253: 320–323.
  31. Lingwood CA. Colocalization of sulfogalactosylacylalkylglycerol (SGG) and its binding protein during spermatogenesis and sperm maturation. Topology of SGG defines a new testicular germ cell membrane domain. *Biochem Cell Biol* 1986; 64:984–992.
  32. Moase CE, Kamolvarin N, Kan FWK, Tanphaichitr N. Localization and role of sulfoglycolipid immobilizing protein 1 on the mouse sperm head. *Mol Reprod Dev* 1997; 48:1–11.
  33. Hogan B, Costantini F, Lacy E. *Manipulating the mouse embryo: a laboratory manual*. Cold Spring Harbor, NY: Cold Spring Harbor Laboratory; 1986.
  34. Attar M, Wong PTT, Kates M, Carrier D, Jaklis P, Tanphaichitr N. Interaction between sulfogalactosylceramide and dimyristoylphosphatidylcholine increases the orientational fluctuations of the lipid hydrocarbon chains. *Chem Phys Lipids* 1998; 94:228–238.
  35. MacDonald RC, MacDonald RI, Menco B, Takeshita K, Subbarao NK, Hu L-R. Small-volume extrusion apparatus for preparation of large, unilamellar vesicles. *Biochim Biophys Acta* 1991; 1061:297–303.
  36. Zalc B, Jacque C, Radin NS, Dupouey P. Immunogenicity of sulfatide. *Immunochemistry* 1977; 14:775–779.
  37. Lingwood CA, Murray RK, Schachter H. The preparation of rabbit antiserum specific for mammalian testicular sulfogalactosylglycerolipid. *J Immunol* 1980; 124:769–774.
  38. Eddy EM, Muller CH, Lingwood CA. Preparation of monoclonal antibody to sulfatoxygalactosylglycerolipid by in vitro immunization with a glycolipid-glass conjugate. *J Immunol Methods* 1985; 81:137–146.
  39. Crook SJ, Stewart R, Boggs JM, Vistnes AI, Zalc B. Characterization of anti-cerebroside sulfate antisera using a theoretical model to analyze liposome immune lysis data. *Mol Immunol* 1987; 24:1135–1143.
  40. Fredman P, Mattsson L, Andersson K, Davidsson P, Ishizuka I, Jeansson S, Mansson JE, Svennerholm L. Characterization of the binding epitope of a monoclonal antibody to sulphatide. *Biochem J* 1988; 251: 17–22.
  41. Gadella BM, Gadella TWJ, Colenbrander B, Van Golde LM, Lopes-Cardozo M. Visualization and quantification of glycolipid polarity dynamics in the plasma membrane of the mammalian spermatozoon. *J Cell Sci* 1994; 107:2151–2163.
  42. Kniep B, Muhlradt PF. Immunochemical detection of glycosphingolipids on thin-layer chromatograms. *Anal Biochem* 1990; 188:5–8.
  43. Van der Pal RHM, Vos JP, van Golde LMG, Lopes-Cardozo M. A rapid procedure for the preparation of oligodendrocyte-enriched cultures from rat spinal cord. *Biochim Biophys Acta* 1990; 1051:159–165.
  44. Gadella BM, Colenbrander B, Van Golde LMG, Lopes-Cardozo M. Boar seminal vesicles secrete arylsulfatases into seminal plasma: evidence that desulfation of seminolipid occurs only after ejaculation. *Biol Reprod* 1993; 48:483–489.
  45. Van Hof't R, van Klompenburg W, Pilon M, Kozubek A, de Kortekool G, Demel R, Weisbeck PJ, de Keruiff B. The transit sequence mediates the specific interaction of the precursor of ferredoxin with chloroplast envelope membrane lipids. *J Biol Chem* 1993; 268:4037–4042.
  46. Brouwers JF, Gadella BM, van Golde LM, Tielens AG. Quantitative analysis of phosphatidylcholine molecular species using HPLC and light scattering detection. *J Lipid Res* 1998; 39:344–353.
  47. Kundu SK. Thin-layer chromatography of neutral glycosphingolipids and gangliosides. *Methods Enzymol* 1981; 72:185–204.
  48. Harlow E, Lane D. *Antibodies: A Laboratory Manual*. Cold Spring Harbor, NY: Cold Spring Harbor Laboratory; 1988.
  49. Tanphaichitr N, Moase C, Taylor T, Surewicz K, Hansen C, Namking M, Bérubé B, Kamolvarin N, Lingwood CA, Sullivan R, Rattana-chaiyanont M, White D. Isolation of antiSLIP1-reactive boar sperm P68/62 and its binding to mammalian zona pellucida. *Mol Reprod Dev* 1998; 49:203–216.
  50. Ward CR, Storey BT, Kopf GS. Activation of a G<sub>i</sub> protein in mouse sperm membranes by solubilized proteins of the zona pellucida, the egg's extracellular matrix. *J Biol Chem* 1992; 267:14061–14067.
  51. Bleil JD, Wassarman PM. Identification of a ZP3-binding protein on acrosome intact mouse sperm by photoaffinity crosslinking. *Proc Natl Acad Sci U S A* 1990; 87: 5563–5567.
  52. Chen S, Cardullo R. Characterization and localization of fluorescent zonae pellucidae on mouse sperm. *Mol Biol Cell* 1994; 5:224a.
  53. Bleil JD, Wassarman PM. Galactose at the nonreducing terminus of O-linked oligosaccharides of mouse egg zona pellucida glycoprotein ZP3 is essential for the glycoprotein's sperm receptor activity. *Proc Natl Acad Sci U S A* 1988; 85:6778–6782.
  54. Legge M. Oocyte and zygote zona pellucida permeability to macromolecules. *J Exp Zool* 1995; 271:145–150.
  55. Familiari G, Nottola SA, Familiari A, Motta PM. The three-dimensional structure of the zona pellucida in growing and atretic ovarian follicles of the mouse: scanning and transmission electron-microscopic observations using ruthenium red and detergents. *Cell Tissue Res* 1989; 257:247–253.
  56. Ahnonkitpanit V, White D, Suwajanakorn S, Kan F, Namking M, Wells G, Tanphaichitr N. Role of egg sulfolipid immobilizing protein 1 (SLIP1) on sperm-egg plasma membrane binding. *Biol Reprod* 1999; 61:749–756.
  57. Gadella BM, Lopes-Cardozo M, van Golde LMG, Colenbrander B, Gadella TWJ. Glycolipid migration from the apical to the equatorial subdomains of the sperm head plasma membrane precedes the acrosome reaction. *J Cell Sci* 1995; 108:935–945.
  58. Topfer-Petersen E, Henschen A. Acrosin shows zona and fucose binding: novel properties for a serine proteinase. *FEBS Lett* 1987; 226: 38–42.
  59. Brown CR, Jones R. Binding of zona pellucida proteins to a boar sperm polypeptide of M<sub>r</sub> 53,000 and identification of zona moieties involved. *Development* 1987; 99:333–339.
  60. Mori E, Baba T, Iwanatsu A, Mori T. Purification and characterization of a 38-kDa protein, SP38, with zona pellucida-binding property from porcine epididymal sperm. *Biochem Biophys Res Commun* 1993; 196:196–202.
  61. Rosen SD, Bertozzi CR. Leukocyte adhesion: two selectins converge on sulphate. *Curr Opin Cell Biol* 1996; 6:261–264.
  62. Law H, Itkonen O, Lingwood CA. Sulfogalactosyl binding protein SLIP 1: a conserved function for a conserved protein. *J Cell Physiol* 1988; 137:462–468.
  63. Larson JL, Miller DJ. Sperm from a variety of mammalian species express  $\beta$ 1,4-galactosyltransferase on their surface. *Biol Reprod* 1997; 57:442–453.
  64. Copley RR, Barton GJ. A structural analysis of phosphate and sulphate binding sites in proteins. *J Mol Biol* 1994; 242:321–329.
  65. Stewart RJ, Boggs JM. A carbohydrate-carbohydrate interaction between galactosylceramide-containing liposomes and cerebroside sulfate-containing liposomes: dependence on the glycolipid ceramide composition. *Biochemistry* 1993; 32:10666–10674.
  66. Iwabuchi K, Yamamura S, Prinetti A, Handa K, Hakomori S. GM3-enriched microdomain involved in cell adhesion and signal transduction through carbohydrate-carbohydrate interaction in mouse melanoma B16 cells. *J Biol Chem* 1998; 273:9130–9138.
  67. Hardy DM, Garbers DL. A sperm membrane protein that binds in a species-specific manner to the egg extracellular matrix is homologous to von Willebrand Factor. *J Biol Chem* 1995; 270:26025–26028.
  68. Tupper S, Wong PTT, Kates M, Tanphaichitr N. Interaction of divalent cations with germ cell specific sulfogalactosylglycerolipid and the effects on lipid chain dynamics. *Biochemistry* 1994; 33:13250–13258.